Iranian Polymer Journal
https://doi.org/10.1007/s13726-026-01730-z

ORIGINAL RESEARCH

Application of artificial neural network (ANN) to predict the curing rate equation parameters of rubber foam

Ali Nikakhtar[1] · Gholam Hossein Zohuri[2] · Ramin Falatooni[3] · Fatemeh Farhmandmoghadam[3]

Received: 6 October 2025 / Accepted: 17 July 2026

Abstract

Rubber foam is one of the materials that is being developed due to its unique properties, such as low density, flexibility, energy absorption ability, etc. Parameters such as compound formulation and vulcanization conditions are affected on these properties. For this reason, kinetic modeling of the vulcanization process is important. In this study, a new method for calculating the parameters which are effect on one of the kinetic models (the Qureshi model) is presented. A model of feed forward back propagation artificial neural network (FF BP ANN) is designed that can predict two model parameters by taking the normalized degree of cure data. The ANN model was trained with the help of this kinetic model data. The capability of the trained ANN was investigated with calculating the error in predicting these parameters. It was found that the parameters were predicted with well accuracy. The experimental data obtained from the rheometer were given as input to the ANN model and the parameters (n and k, the degree and rate constant respectively) related to these data were calculated. This work was also done using the conventional curve fitting method. A comparison between the experimental data reviled that the results obtained from the curve fitting method and the new method presented in this work provides appropriate results in predicting the parameters.

Graphical abstract

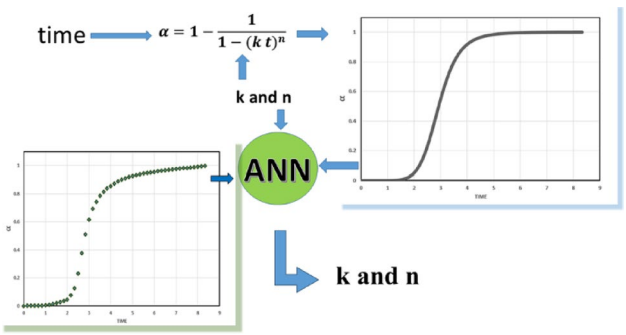

Keywords Artificial neural network (ANN) · Vulcanizations process · Modeling · Model parameters · Rubber foam

Introduction

The progress of science and technology and the development of societies have led to an increasing need for all materials, especially rubber foams. These materials have properties such as energy absorption, thermal insulation, sound insulation, lightness, flexibility, abrasion resistance and sufficient tensile strength, etc. [1, 2]. Several parameters that affect the microscopic structure of these materials

✉ Ali Nikakhtar
anikakhtar@birjand.ac.ir

1 Department of Chemistry, Faculty of Science, University of Birjand, Birjand, Iran

2 Department of Chemistry, Faculty of Science, Ferdowsi University of Mashhad, Mashhad, Iran

3 Engineering Department, Ayegh Khodro Toos (AKT) of Part Lastic Industrial Group, Mashhad, Iran

Published online: 25 August 2026

are directly related to their physical and mechanical properties [3]. These parameters are divided into two categories, the first category includes formulation-related parameters such as the amount and type of ingredients used in the compound, and the second category includes parameters related to processing conditions such as temperature, pressure, curing time, number of steps, and their sequence [4, 5]. Kinetic modeling of the curing process is very important to investigate these parameters and manufacture efficient products.

To produce foam, two reactions occur simultaneously: gas generation, which causes the formation of cells, and cross-linking, which stabilizes them by creating a three-dimensional structure. Even if these two series of chemical reactions occur independently, their effect on the physical properties of the medium makes them dependent on each other, and therefore it is important to know their progress relative to each other [6].

Curing process

The most common method for determining the curing properties of a compound is the use of an ODR, oscillation disk rheometer [7, 8]. In this device, the shear load required to vibrate a disk at a constant temperature which is measured as a function of time. The result is an isothermal curing curve, which is plotted as torque versus time. From the curing curves, properties such as minimum modulus, maximum modulus, induction time, and best curing time can be directly extracted, and several derivative-dependent properties such as curing rate ratio, curing rate coefficient, degree of crosslinking, and thermoplasticity can be extracted [9].

Accelerated sulfur curing consists of three stages. In the pre-curing stage, zinc oxide, activator, reacts with stearic acid, accelerators, and sulfur to produce precursors for crosslinking. These reactions delay the formation of sulfur crosslinks. In the curing stage, the rate of sulfur crosslink formation increases, and then in the post-curing stage, due to the consumption of reactive species, the rate of crosslink formation stops and even breaks the crosslinks under certain conditions [10].

Since the accelerated curing process consists of three stages and these stages are the result of a large number of reactions, modeling the process is very difficult [11]. Various models have been reported on the subject of curing. These models include two categories: mechanistic models and phenomenological models (empirical models) [12]. Coran model is one of the first established mechanistic models presented. This model was later modified by Ding and Leonov. In this model, all of the three process stages are considered and are include six related reactions. The rate equations of these reactions form a system of related differential equations that include all of the six parameters (rate constants) [13]. Since analytical solution of this system of differential equations is not possible, it is solved by simplifying the differential equations.

Other models in this category include the Milano model [14–16] and the Henn model [17], which are mostly used for the curing and post-curing stages [18]. Another group of mechanistic models are population equilibrium models, in which a large number of possible reactions are considered. The rate equations for these reactions form a system of differential equations that can only be solved numerically [11]. Phenomenological models are models in which a mathematical function with a number of parameters is fitted nonlinearly to the experimental data and the best values for the parameters are calculated [18–21].

The most common of these relationships is similar to the nth-order reaction kinetic model, Eq. 1

$$\frac{da}{dt} = k(1-a)^n \tag{1}$$

where α is the normalized degree of cure, n and k are the degree and rate constant of the reaction, respectively. The temperature dependence of the rate constant follows the Arrhenius equation. The value of n obtained for this equation is reported to be 0.2, the maximum rate of the process with this model is at time zero, while the maximum rate based on experimental data corresponds to times which is greater than zero. This is a characteristic of autocatalytic processes. Piloyan et al. [19] presented a more complex model and this model was later used by Kamal et al. to describe the curing of thermosetting polymers such as polyesters and polyepoxy [20–22]. Isayo et al. used this model for rubber, Eq. 2 [22]

$$\frac{da}{dt} = k\, a^m (1-a)^n \tag{2}$$

where n and m are two parameters similar to the degree of reaction. By integrating these relations, equations can be obtained that explicitly calculate the normalized degree of cure. Other works in this field include the Kamal equation Eq. 3 [20]

$$\frac{da}{dt} = \frac{n}{k}\,(t-t_i)^{-(1+n)}\, a^2 \tag{3}$$

By integrating this relationship, Eq. 4 is obtained

$$\mathrm{a} = \frac{k\,(t-t_i)^n}{1+k\,(t-t_i)^n} \tag{4}$$

In these relations, t_i is the pre-curing time. This equation has been modified by Ghoreishy et al. (Eq. 5) [23, 24]

$$a = A_1 - \frac{A_1 - A_2}{1 + (k\,t)^n} \tag{5}$$

where A_1 and A_2 are correspond to the maximum and the minimum curing values, respectively.

This equation can be used for all of three types of conventional vulcanization (CV), semi efficient vulcanization (SEV), and efficient vulcanization (EV) curing systems and MDR and ODR curing curve. In general, this equation is applicable to any curing curve that has pre-curing and curing stages and has a small revers process in the post curing stages.

Estimating the parameters of simulation models to fit experimental data is one of the key challenges in science and engineering for modeling complex systems. Various methods have been developed for this purpose. These methods are divided into two categories: classical methods and metaheuristic algorithms classical methods are often based on the minimization of the sum of squared errors (least-squares) and are suitable for linear or nonlinear models. The ordinary least squares method and the nonlinear least squares method have been used to estimate the parameters of models in hydrology and in batteries. The advantages of this method are simplicity and speed.

The Levenberg-Marquardt method uses a hybrid algorithm that uses two gradient descent methods and the Newton method is used to extract parameters from many models, such as electronic models. This method optimizes all parameters simultaneously [25]. BFGS (Broyden–Fletcher–Goldfarb–Shanno) method operates on the basis of mathematical gradients (used for the nonlinear Muskingum model) and can calculate parameters with the least number of iterations. It also analyzes sensitivity to initial values [26].

Metaheuristic and global methods are suitable for nonlinear and complex models. These methods use a global search to avoid local optima. They are often used in hydrology, solar cell and tire models. The genetic algorithm method is in this category and its advantages are fast convergence without requiring any knowledge of the model [27]. The particle swarm optimization method, PSO, solves the problem of getting stuck in local optima by combining analytical algorithms [28]. Other methods in this category include MCMC, Kalman filter and adjoint algorithms [29, 30]. Choice of method depends on the complexity of the model, the type of data, and the area of application.

Artificial neural networks

Advances in artificial intelligence and machine learning in the past decades have shown that ANN are very effective tools for modeling complex processes [31]. Their great advantage is that they can model any complex nonlinear relationship between process variables without prior knowledge of the process or system models. For example, the structure of the ANN model was studied to predict the final curing time of 11 compounds at different temperatures in a tire model [32]. In a subsequent study by the same authors, three different types of ANN model and an adaptive neuro-fuzzy inference system (ANFIS) with the ANN model architecture and the ANN model learning technique were successfully used to predict the optimal curing time of another 10 rubber compounds at different curing temperatures [33].

Lubura et al. developed a fast and accurate ANN model to predict the rheological curing curve of NR/SBR blends at different curing temperatures [34]. In another study, the effects of filler content as well as temperature on the maximum and the minimum torque values, pre cure time, and optimal curing time were modeled using the ANN. The network was built based on the regression principle, and the errors were not more than 5% [35].

Here, a new method, distinct from the above-mentioned methods, is proposed for calculating the parameters of a kinetic model. This method can be applied to both mechanistic and phenomenological models. The aim of this research is to estimate the parameters related to the Qureshi model. For this purpose, first, the rheometric data of the torque were extracted in terms of time. Because the experimental data are torque with large range of values, for a more efficient optimization during the training the data obtained from the rheometer were normalized according to the Eq. 6:

$$a = \frac{M - M_{min}}{M_{Max} - M_{min}} \tag{6}$$

where α is normalized degree of cure and M_{Max}, M_{min} and M are the minimum torque, the maximum torque and torque at any time respectively. In the Eq. 5, A_1 and A_2 are related to the minimum torque and the maximum torque respectively, and were considered to be zero and one respectively.

Then an ANN model based on Eq. 7 was designed to calculate the values of these two parameters by taking the normalized degree of cure data. This network was trained with the help of the data obtained from the Eq. 7. Following to that by entering the experimental data as input, the values of n and k are calculated and estimated.

$$a = 1 - \frac{1}{1 + (k\,t)^n} \tag{7}$$

Experimental

Materials

The materials used in this study are listed in Table 1. Due to the amount of sulfur and the accelerators, this vulcanization was of the (EV) type, which is made in the production line and is used as a sound absorber.

The ingredients are mixed at 60 °C. SBR (styrene butane rubber) is softened using a Banbury. Then, stearic acid and zinc oxide are added until a homogeneous mixture is obtained. Paraffin oil and carbon black (N330) are gradually added. Following to that Azodicarbonamid (ADC), Mercaptobenzothiazole disulfide (MBTS) and Tetramethyl thiuram disulfide (TMTD) the accelerators are added, and in the last step, sulfur is added. The sample is then kept at ambient temperature to cool.

The compound was studied using an ODR rheometer at temperatures of 150, 160, 170 and 180 °C.

Calculation method

To predict the parameters of the Eq. 7, a multilayer feed-forward back-propagation artificial neural network (FF-BP-ANN) model is developed. The ANN structure consists of an input layer, a hidden layer, and an output layer. The input data are the experimental values of the normalized degree of cure related to a curing curve at specific times. 51 data (normalized degree of cure) with a time interval of 10 s between two measurements constitute the input values, and output of the data are the two parameters of n and k of the Eq. 7 related to the same curing curve.

The role of the input layer is to transfer data to the hidden layer. Each neuron in the hidden layer and the output layer consists of an input, weight, bias, summing junction transfer function, and output. Each element of the input data matrix (p) (matrix 8) is at the input to each hidden neuron multiplied by its weight matrix $IW_{j,i}^{1,1}$ and make weighted inputs. These weighted inputs of individual s^1 neurons j of the hidden layer are mutually summed in their summing junctions and the bias b_j^1 of the current neuron j, representing a constant external input with a value of 1 multiplied by its weight, is added to the result [36].

$$p = \begin{pmatrix} x_{11} & x_{12} & x_{13} & . & . & . & x_{1N} \\ x_{21} & x_{22} & x_{23} & . & . & . & x_{2N} \\ x_{31} & x_{32} & x_{33} & . & . & . & x_{3N} \\ . & . & . & . & . & . & . \\ . & . & . & . & . & . & . \\ . & . & . & . & . & . & . \\ x_{511} & x_{512} & x_{513} & . & . & . & x_{51N} \end{pmatrix} \tag{8}$$

The weighted sum of inputs and bias of each neuron j of the hidden layer generates the net input of the hidden neuron Eq. 9.

$$n_j^1 = \sum_{i=1}^{51} IW_{j,i}^{1,1} p_i + b_j^1, \quad j = 1,2,3,\ldots,s^1 \tag{9}$$

Leading to its activation, which is then inserted into the non-linear transfer function (log) producing its output in the form, Eq. 10.

$$a_j^1 = logsig\left(n_j^1\right) = \frac{1}{\{1 + exp(-n)\}} \tag{10}$$

Subsequently, the net input of the output layer (Eq. 11) is inserted into the linear transfer function which will generate its output signal (Eq. 12).

$$m_k^2 = ?_{j=1}^{s^1} IW_{k,j}^{2,1}\, a_j^1 + b_k^2, \qquad k = 1,2 \tag{11}$$

$$a_k^2 = purelin\ \left(m_k^2\right) = m_k^2 \tag{12}$$

The output data matrix is as follow (matrix. 13):

$$\boldsymbol{a} = \begin{pmatrix} n_1 & n_1 & n_3 \ldots & n_N \\ k_1 & k_2 & k_3 \ldots & k_N \end{pmatrix} \tag{13}$$

The upper indexes 1 and 2 as the hidden and output layer of the network are marked with superscripts 1 and 2, respectively. The subscript i denotes the elements of the input signal, the subscript j denotes the hidden layer neurons, and the subscript k represents a single neuron of the ANN output layer. The FF-BP-ANN architecture is designed as fully connected.

The model shown in Fig. 1 estimates the values of the two parameters of n and k by giving 51 points of experimental data. In order for the network to predict correctly, the network needs to be trained. In the training process, the weight matrix (W) and the biases (b) are determined. The training process is as follows: first, initial values are assigned to the weight and bias matrixes with the help of random numbers, then the training data is given to the network and output of

Table 1 Part of ingredients adopted in the formulation of the prepared sample

Ingredients	SBR	Stearic acid	ZnO	Sulfur	TMTD	MBTS	ADC	Carbon Black
phr	100	5	5	1	4	14	7	35

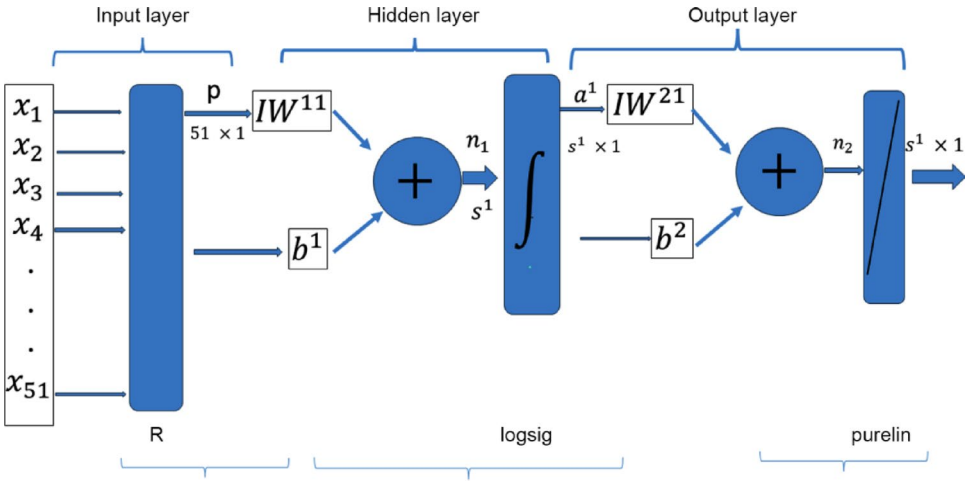

Fig. 1 Scheme of multilayer FF-BP-ANN

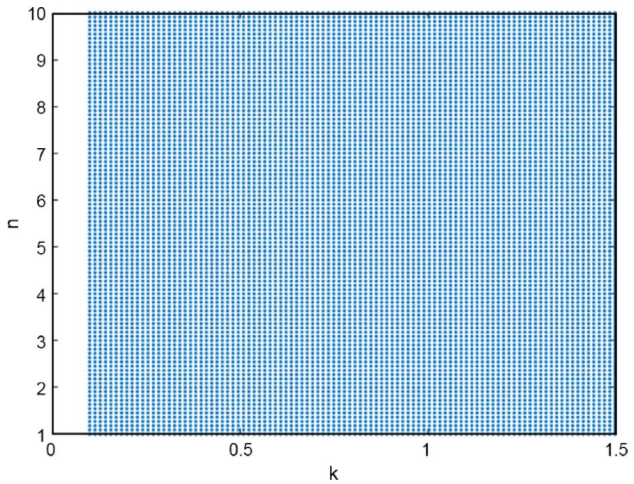

Fig. 2 Data set used to train the network

the network is calculated. Now, the difference between the network output and the real data is obtained and the weights are modified based on this difference value by the training algorithm. Thus, the first iteration (epoch) is performed.

In the second epoch, the training data is fed back to the network whose weights were modified in the first step, and the difference between the network output and the actual data is calculated. The weight and the bias matrix are modified for the second step. These epochs continue until the best match between the output data and the actual values is achieved. The mean square error (MSE) between the training data and the predicted values from the network decreases at each epoch. The MSE decreases with increasing number of epochs. This measure indicates the effectiveness of the training.

The ANN network model needs to have the ability to estimate the two parameters of n and k by taking the normalized degree of cure data at specific times (i.e., α and t are specified). Therefore, to construct the training data, a set of n and k values was first obtained in this way. At temperature 160 °C, the experimental data was given to the curve fitting section of the MATLAB software, and the prediction of these two parameters of k and n were 0.5404 and 8.476, respectively. Based on these obtained values, the ranges of n and k were determined as ($1<n<10$) and ($0.1<k<1.5$), respectively.

Each of these ranges were divided into M parts and for the pair of the parameters n and k, the number of M×M=N states were considered. Figure 2 shows the number of these states for M=100. The coordinates of each point in this figure are one state of the pair of the parameters n and k, which represents one of the columns of the data matrix (13). The processing time was considered to be 500 s. This time range was divided into 50 parts, so the time corresponding to the points used in all the diagrams is as follows:

$$t = 0\ ,\ 10\ ,\ 20\ ,\ 30\ ,\ 40\ ,\ .\ .\ .\ ,500 \tag{14}$$

By substituting the n and k in the Eq. 7, the normalized degree of cure data (α) at specified times (Eq. 14) was calculated for each of the n and k. Now, the normalized degree of cure data was given as input, matrix 8, and its corresponding n and k as target, matrix 13, to the ANN model and training was performed with this data.

By entering of the n and k in the Eq. 7 at the specified times, (Eq. 14) the normalized degree of cure data for each of them are obtained. Now the normalized degree of cure data (α) as input, matrix data 8, and its corresponding n and k as target, matrix 13, were given to the ANN network model and training was carried out with these data.

Results and discussion

The ANN network model must have the ability to accurately predict both of the parameters of n and k by taking the normalized degree of cure data that is calculated using

the Eq. 7. In addition, this network must be able to take the experimental data and estimate the parameters of n and k. Then, if these obtained parameters, n and k, are put into the Eq. 7, the generated data should be in good agreement with the experimental obtained data. These two abilities are further discussed as follow.

Application of ANN on model data

Figures 3, 4 and 5 show the resulted errors in the various quantities predicted with the network. These errors are the differences between these quantities and what was initially considered. The points marked in Fig. 2 correspond to the N assumed states of the n and k that the network is expected to be able to predict. Here, the error values are indicated by colors and the colored bars next to the graph show the error values associated with each color. Thus, the constructed color surface shows the performance of the network for the n and k corresponding to it. Figures 3, 4 and 5 show the error frequency distribution values among the points of the resulting set of the N points marked in Fig. 2. In the first step, the both values of n and k corresponding to these points are given to Eq. 7 and the normalized degree of cure (x_i) was calculated. In the second step the normalized degree of cure values given to the ANN and the values of the k_p and the n_p were obtained. By using Eqs. 15 and 16 the relative error value in both of the n and k was calculated.

$$En = \frac{n_p - n}{n} \times 1000 \tag{15}$$

$$E_k = \frac{k_p - k}{k} \times 1000 \tag{16}$$

In the third step, both of the k_p and the n_p were given to the Eq. 7 and the normalized degree of cure r_i were calculated. By comparing these values with the normalized degree of cure (x_i) which was calculated in the first step, the error value in the network prediction was obtained using Eq. 17.

$$RMSE = \sqrt{\frac{\sum_{i=1}^{N}(x_i - r_i)^2}{N}} \times 1000 \tag{17}$$

Figure 3 shows effect of the training process on the relative error in the prediction of k obtained by the network. Figure 3a corresponds to a case with.

MSE $= 10^{-3}$. In this figure, although the error values are low in the large n, the color bar corresponding to the errors shows a large range between −800 and 200. By comparing Fig. 3b with 3a where $MSE = 10^{-6}$, it is clear that not only the error range has been reduced, but the fluctuations in the level have also decreased. This feature guarantees the accuracy of the results obtained by the network. With increasing epochs in the training process, the MSE reduction trend has almost stabilized and reached to $MSE = 8 \times 10^{-9}$. Figure 3c, which corresponds to this case, shows that the errors

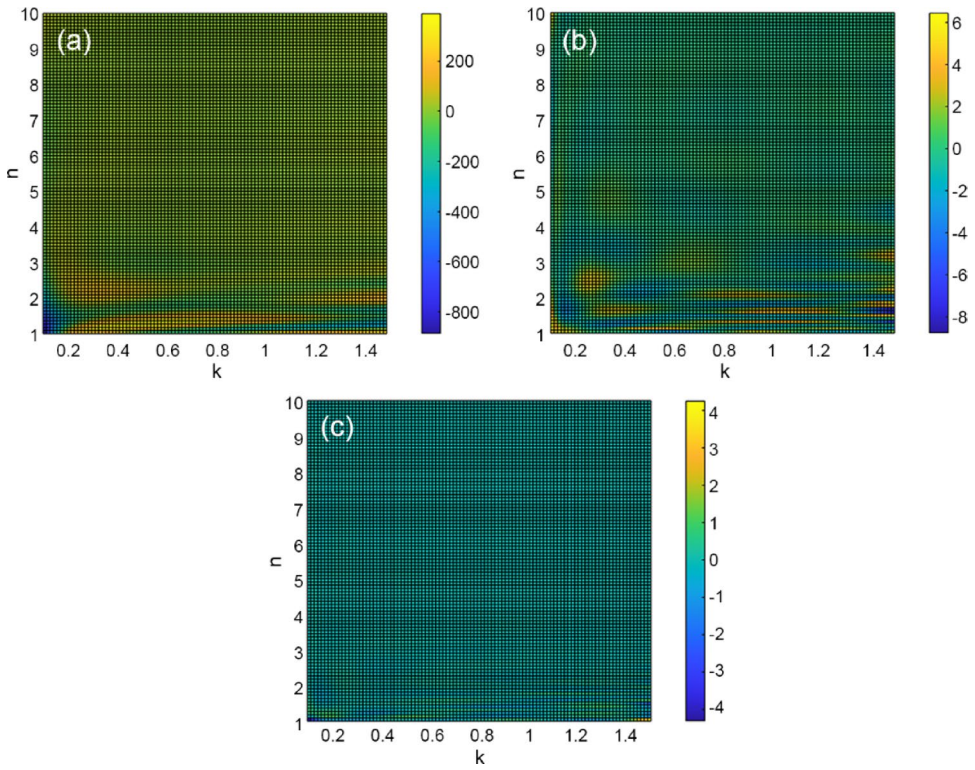

Fig. 3 Effect of the training progress process on the errors resulting from the prediction of the k at three MSE values: **a** 1×10^{-3}, **b** 1×10^{-6}, **c** 8×10^{-9}

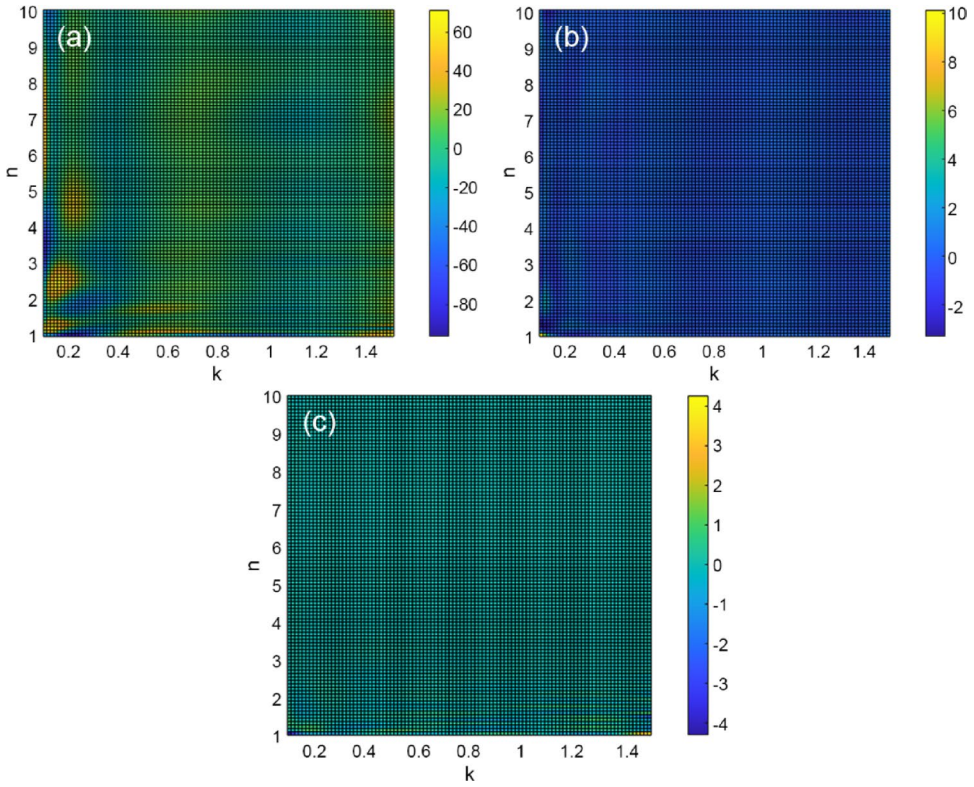

Fig. 4 Effect of the training progress process on the errors resulting from the prediction of the n at three MSE values: **a** 1×10^{-3}, **b** 1×10^{-6}, **c** 8×10^{-9}

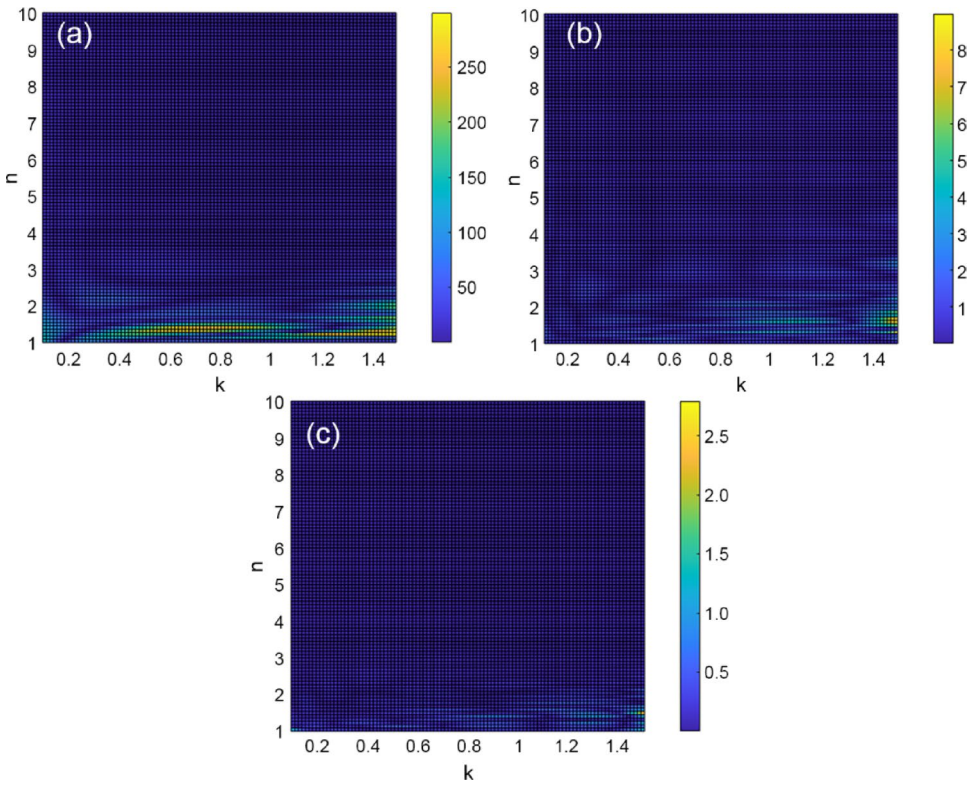

Fig. 5 Effect of the training progress process on the errors resulting from the prediction of the progress process at three MSE values: **a** 1×10^{-3}, **b** 1×10^{-6}, **c** 8×10^{-9}

have become very small and there is very good uniformity almost throughout the entire range.

Figure 4 shows effect of the training process on the relative error in the prediction of the n obtained by the network. Here too, the error range in the Fig. 4a and b includes negative and positive values, and in the Fig. 3c the values are only positive and are in a small range, and very good uniformity is observed almost throughout the entire range. The distribution of errors in the n is different from what was observed in the case of the k, which indicates that the training process predicts these two quantities independently.

Figure 5 shows effect of the training process on the prediction of the normalized degree of cure by the network. The criterion used here is the RMSE quantity, which shows the error amount in predicting the normalized degree of cure in each of the cases. The general trend of the Fig. 5a, b and c is similar to the Figs. 3 and 4, in that the error range and its fluctuations decrease as the training process progresses. Of course, these observations are expected because the errors in the Fig. 5 are the result of the error in predicting both of the k and n. The noteworthy point is that the Figs. 3 and 5 are more similar to each other, so the parameter of the k is more decisive than the n in the error resulting from predicting the normalized degree of cure.

Table 2 shows the characteristics of the neural network model designed to predict the accelerated curing curve of sulfur. This network is used to calculate the parameters of the Eq. 7. Due to the simplicity of the shape of the curing curve, the network with one hidden layer is suitable for this task. In this network model, the transfer function in the hidden layer was selected to be of the logarithmic type, whose symbol in the MATLAB software is (LOGSIG). This function is very similar to the curing curve and, like the curing curve its range is between zero and one. The transfer function in the output layer is assumed to be a linear function so that the weights of the first layer have the same proportion in the output data. This function is introduced in the MATLAB software with the symbol (pureline). The data time of each curve was considered every 10 s to achieve the required accuracy. Another factor that affects the performance of the network is the number of data used for the training. Here, there is no limit on the number of the data, and therefore 10,000 data sets were used for the training. This number ensures proper learning for the network. By entering the training data, the weights and biases are modified and the MSE quantity is calculated for each of the epoch. By repeating these calculations and increasing the number of the epochs, the MSE quantity decreases. As seen in the Figs. 3, 4, 5 and 6, suitable results were obtained for the and the best result was obtained for the MSE < 10^{-8}.

Table 2 Characteristics of the ANN used to predict the parameters of Eq. 7

Type of neural network	FF-BP-ANN
Number of neurons in output layer	2
Number of hidden layers	1
Number of neurons in hidden layer	51
Train Function	Levenberg Marcart (TRINLM)
Adaption learning function	LEARNGDM
Performance function	Mean square error MSE
Transfer function hidden layer	Logarithm function (logsig)
Transfer function output layer	Linear function (purlin)
Number of input data	51
Number of output data	2
Number of data for training	10,000
Number of output data	2

Application of ANN on experimental data

Torque versus time in the rubber compound curing process at temperatures range of 140 to 180 °C is shown in Fig. 6. Increasing the temperature raised rate of the reactions, as a result, the pre-curing time decreases and the rate of the curing process increases, which results in an increase in the slope of the curve in the curing stage. Increasing the temperature due to decreasing the process time causes a decrease in the density of crosslinks, and as a result, the final torque decreases.

As mention for more efficient optimization the torque were normalized into the (0, 1) interval according to the Eq. 12 and the normalized degree of cure is illustrate in the Fig. 7.

To prove accuracy of this method, it is necessary to compare the results of a conventional method with the ANN results. For this purpose, in the first step, the normalized degree of cure data in terms of time was given to the curve fitting section in the MATLAB software, and by fitting the data by the Eq. 7, the two parameters of n and k were obtained for temperatures range from 150 to 180 °C, Table 2. Afterword, the values of n and k were substituted in the Eq. 7 and the normalized degree of cure at the specified times (Eq. 14) was obtained. By comparing this normalized degree of cure values with the experimental values, the MSE quantity related to each of the temperature was obtained. These values are also reported in Table 2.

In the second step, the experimental data was given to the trained network model with the lowest MSE (best performance). The two parameters of n and k were obtained for the temperatures range from 150 to 180 °C. By repeating the same calculations, the MSE fitting method related to the ANN prediction was obtained, which is also reported in the Table 3. By comparing the values of n, k and MSE using the two methods, it is clear that the ANN provides very close results to the conventional fitting method. In Table 3, relative error in prediction of the k and n is reported relative to the value of the curve fitting procedure. The maximum error

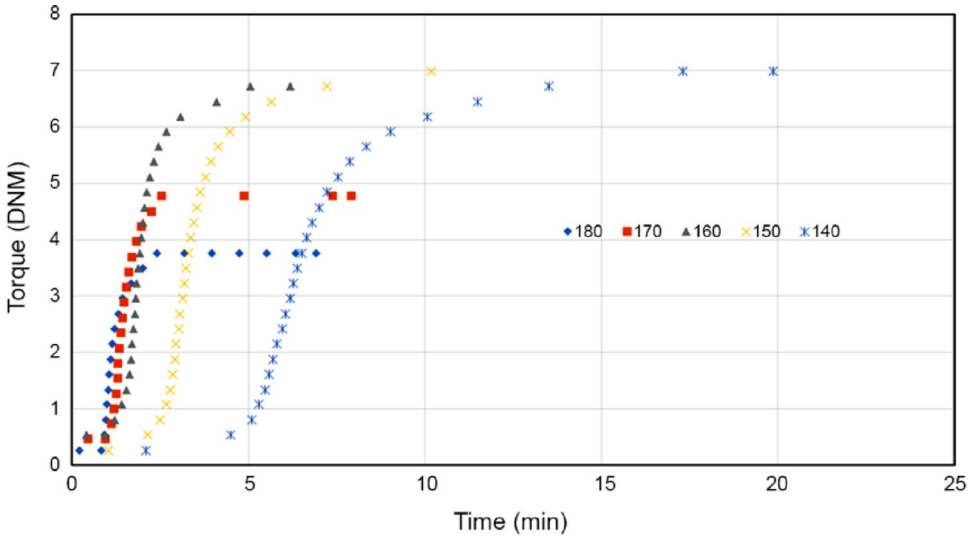

Fig. 6 Curing diagram obtained from the rheometer device

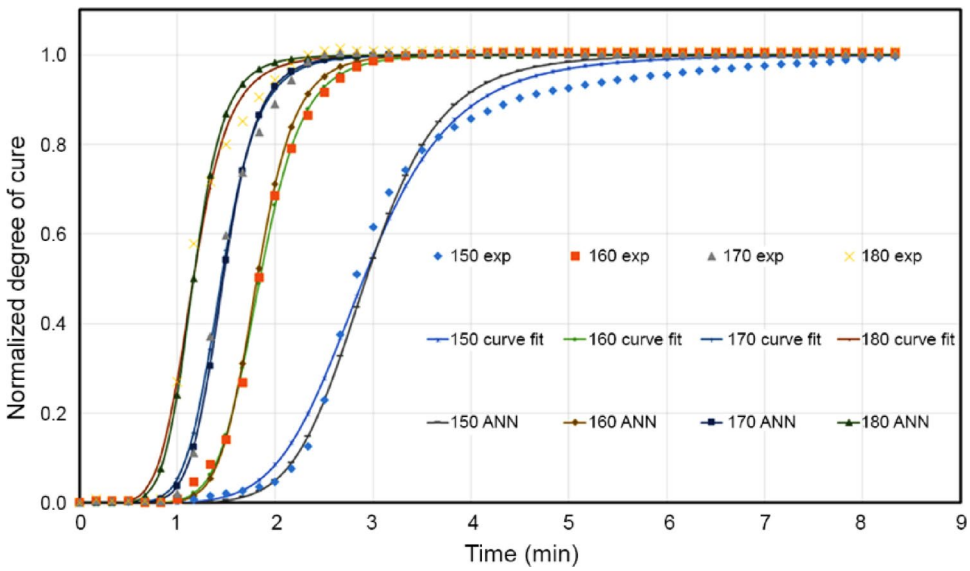

Fig. 7 Comparison of the experimental fitting methods data and the neural network

Table 3 Comparison of the n, k values and the MSE at different temperature (ºC)

		180	170	160	150
Curve fit	k	0.858	0.6889	0.5422	0.3444
	n	6.398	7.727	8.362	6.376
	MSE	5.16E−04	1.70E−04	8.48E−05	9.79E−04
ANN	k	0.8455	0.6852	0.5392	0.3314
	n	5.6270	7.2603	8.4351	7.7031
	MSE	6.37E−04	1.99E−04	9.41E−05	1.91E−03
	Relative error in k	− 1.4568	− 0.53708	− 0.55330	− 3.7746
	Relative error in n	− 12.050	− 6.0398	0.87419	20.813

in the k and n is at temperature of 150 °C. In this temperature, both of the methods have the maximum MSE which corresponds to the deficiency of the Eq. 7. The suitability of the errors in the two methods indicates the accuracy of this method.

The Experimental and the prediction obtained data from the fitting method and the ANN model is compared (Fig. 7). The comparison shows that the data of these two simulation methods are match to each other. Therefore, not only, the performance of the neural network is similar to the fitting method, which indicates the accuracy of this new method but also the difference with the experimental data is related to the defect in the Eq. 7.

Based on what was mentioned in the reference, the parameter k has an Arrhenius relationship with temperature $((k = Aexp(\frac{-E}{RT})))$. The result shows the ln(k) is a linear graph in terms of the1/T $((\ln(k) = -5869.8\frac{1}{T} + 12.839)$

) and $R^2 = 0.9674$. The dependence of n on temperature is a characteristic of the compound during the curing process. This equation can be linear, second degree, or other form as reported [23, 37]. For this experimental data, the relationship is of the second order ($(n = -0.0059T^2 + 5.1077T - 1094.8)$) with R^2 = 0.9753.

Conclusion

In this study, a new method for calculating model parameters related to accelerated sulfur curing process is described. So far, neural networks have not been used for this task, and in fact, this is a new application of neural networks. By this method we have been able to calculate the parameters of a model. Its best advantage is that it does not require an explicit mathematical function for calculation. Although here the work is done with the help of an explicit mathematical function to make a comparison with the conventional method, this method does not have this limitation. Here it is clear that in order to achieve good results, it is necessary to proceed with the training process until the MSE quantity is less than 1×10^{-8}. Comparing the results of this method with experimental data and the fitting method, it was found that similar answers can be obtained with a good network.

Acknowledgements The authors sincerely appreciate and thank the managers of Birjand University, Ayegh Khodro Toos (AKT) of Part Lastic Industrial Group and Part Lastic Industrial Group Innovation and Acceleration Center for their cooperation in conducting this research.

Funding This research received no external funding.

Declarations

Conflict of interest The authors declare no conflict of interest.

Informed consent Not applicable.

References

1. Rostami-Tapeh-Esmaeil E, Rodrigue D (2023) Morphological mechanical and thermal properties of rubber foams: a review based on recent investigations. Materials 16:1934. https://doi.org/10.3390/ma16051934
2. Rostami-Tapeh-Esmaeil E, Vahidifar A, Esmizadeh E, Rodrigue D (2021) chemistry, processing, properties, and applications of rubber foams. Polymers 13:1565. https://doi.org/10.3390/polym13101565
3. Vahidifar A, Khorasani SN, Park CB, Khonakdar HA, Reuter U, Naguib HE, Esmizadeh E (2016) towards the development of uniform closed cell nanocomposite foams using natural rubber containing pristine and organo-modified nanoclays. RSC Adv 6:53981–53990
4. Esmizadeh E, Vahidifar A, Rostami E, Nouri Khorasani Z (2001) effect of high-temperature curing on the crosslink structures and dynamic mechanical properties of gum and N330-filled natural rubber vulcanizates. Polym Test 20:925–936. https://doi.org/10.1016/S0142-9418(01)00035-6
5. Fan RL, Zhang Y, Li F, Zhang YX, Sun K, Fan YZ (2001) Effect of high - temperature curing on the crosslink structures and dynamic mechanical properties of gum and N330-filled natural rubber vulcanizates. Polym Test 20:925-936.
6. Schaible T, Bonten C (2024) Prediction of the bubble growth behavior by means of the time-, temperature-, pressure-and blowing agent concentration-dependent transient elongational viscosity function of polymers. Polymers 16:1213. https://doi.org/10.3390/polym16091213
7. Arrillaga A, Zaldua AM, Atxurra RM, Farid AS (2007) Techniques used for determining cure kinetics of rubber compounds. Eur Polym J 43:4783–4799
8. Jabez IKL, Das U, Gopal AS (2017) Oscillatory disc rheometer: an important quality assurance tool to assess the shear modulus of natural rubber in flex seals of large rocket motor. J Elastomers Plast 49:650–664
9. Hopmann C, Schmitz M (2020) Data acquisition and process monitoring as enabler for Industry 4.0. Plast Ind 4:11–73
10. Ciesielski A (1999) An introduction to rubber technology. iSmithers Rapra publishing
11. Ghosh P, Katare S, Patkar P, Caruthers JM, Venkatasubramanian V, Walker KA (2003) sulfur vulcanization of natural rubber for benzothiazole accelerated formulations: from reaction mechanisms to a rational kinetic model. Rubber Chem Technol 76:592–693
12. Khang T, Ariff Z (2012) Vulcanization kinetics study of natural rubber compounds having different formulation variables. J Therm Anal Calorim 109:1545–1553. https://doi.org/10.1007/s10973-011-1937-3
13. Ding R, Leonov A (1996) A kinetic model for sulfur accelerated vulcanization of a natural rubber compound. J Appl Polym Sci 61:455–463
14. Milani G, Milani F (2012) Comprehensive numerical model for the interpretation of cross-linking with peroxides and sulfur: chemical mechanisms and optimal vulcanization of real items. Rubber Chem Technol 85:590–628
15. Milani G (2013) Effective GA approach for a direct evaluation of reaction kinetic within EPDM accelerated sulphur crosslinking. J Math Chem 51:465–491
16. Milani G, Milani F (2017) Comprehensive kinetic numerical model for NR and high-cis poly-butadiene rubber blends. Chem Eng Trans 57:1495–1500
17. Han IS, Chung CB, Kang SJ, Kim SJ, Jung HC (1998) A kinetic model of reversion type cure for rubber compounds. Polym Korea 22:223–230
18. Leroy E, Souid A, Deterre R (2013) A continuous kinetic model of rubber vulcanization predicting induction and reversion. Polym Test 32:575–582
19. Piloyan G, Ryabchikov O, Novikova OS (1966) Determination of activation energies of chemical reactions by differential thermal analysis. Nature 212:1229–1229
20. Kamal M, Sourour S (1973) Kinetics and thermal characterization of thermoset cure. Polym Eng Sci 13:59–64
21. Kamal M (1974) Thermoset characterization for moldability analysis. Polym Eng Sci 14:231–239. https://doi.org/10.1002/pen.760140312
22. Isayev A, Deng J (1988) Nonisothermal vulcanization of rubber compounds. Rubber Chem Technol 61:340–361
23. Rafei M, Ghoreishy MHR, Naderi G (2009) Development of an advanced computer simulation technique for the modeling of

rubber curing process. Comput Mater Sci 47:539–547. https://doi.org/10.1016/j.commatsci.2009.09.022
24. Ghoreishy MHR (2016) A state-of-the-art review on the mathematical modeling and computer simulation of rubber vulcanization process. Iran Polym J 25:89–109
25. Fischer A, Izmailov AF, Solodov M (2024) The Levenberg–Marquardt method: an overview of modern convergence theories and more. Comput Optim Appl 89:33–67
26. Head JD, Zerner MCJC (1985) A Broyden—Fletcher—Goldfarb—Shanno optimization procedure for molecular geometries. Chem Phys Lett 122:264–270
27. Garcia S, Garnier B, Jarny Y (1999) Simultaneous estimation of kinetic parameters using genetic algorithms. in Inverse Problems in Engineering: Theory and Practice: 3rd Int. Conference on Inverse Problems in Engineering
28. Zhang Y, Wang S, Ji G (2015) A comprehensive survey on particle swarm optimization algorithm and its applications. Math Probl Eng 1:931256
29. Cotter SL (2010) Applications of MCMC methods on function spaces. University of Warwick
30. Courtier P, Derber J, Errico R, Louis JF, Vukićević T (1993) Important literature on the use of adjoint, variational methods and the Kalman filter in meteorology. Tellus A 45:342–357
31. ArulRaj K, Karthikeyan D, Narmatha D (2021) A view of artificial neural network models in different application areas. In: E3S Web of Conferences. EDP Sciences 287:03001
32. Karaağaç B, İnal M, Deniz V (2009) Artificial neural network approach for predicting optimum cure time of rubber compounds. Mater Des 30:1685–1690
33. Karaağaç B, İnal M, Deniz V (2012) Predicting optimum cure time of rubber compounds by means of ANFIS. Mater Des 35:833–838
34. Lubura JD (2021) Prediction of rubber vulcanization using an artificial neural network. Hemijska industrija 75:277–283
35. Kopal I (2022) A generalized regression neural network model for predicting the curing characteristics of carbon black-filled rubber blends. Polymers 14:653
36. Beale MH, Hagan MT, Demuth HBJUSG (2010) Neural network toolbox for use with MATLAB. MathWorks 4:77–81
37. Nikakhtar A, Ziatbar A, Kamkar M (2024) Phenomenological modeling of accelerated sulfur vulcanization process of radial tire belt compound. Iran Rubber Ind 28:71–85